

New Data on the Geological Structure of the Junction between the Cape Verde Seamount and the Cape Verde Basin, Central Atlantic

S. G. Skolotnev, A. A. Peive, N. N. Turko, N. V. Tsukanov, L. A. Golovina, V. N. Efimov, A. E. Eskin, V. Yu. Lavrushin, V. V. Petrova, and N. L. Chaplygina

Presented by Academician Yu. M. Pushcharovsky August 25, 2005

Received September 1, 2005

DOI: 10.1134/S1028334X06020140

The regions of conjugation of continental rise with abyssal oceanic basins at the margins of the Atlantic—a transitional zone between continental and oceanic lithospheres—are still poorly studied in geological terms. In the course of expeditions conducted by the Geological Institute (Moscow), the structure of this zone was studied at the continental slope of Africa, south of the Cape Verde Islands. In this area, the continental rise widens sharply making up a near-latitudinal promontory that divides the abyssal Cape Verde Basin in the south and the Canary Basin in the north. The study area is situated in the pinchout area of the system of transform fracture zones (TFZ) located south of the Fifteen Twenty TFZ [1, 2]. The near-latitudinal linear ridges and troughs on the bottom of the Cape Verde Basin are the eastern flanks of the Vema, Doldrums, Arkhangelsky, and Vernadsky TFZs of the Mid-Atlantic Ridge. Near the continental slope of Africa, these TFZs are cut off by the WNW-trending escarpment (Fig. 1). The bathymetric survey of a local area in the deepwater Cape Verde Basin that adjoins the southern margin of the Cape Verde Seamount (Figs. 1, 3) was carried out during Cruise 22 of the R/V *Akademik Nikolai Strakhov* in 2000. We have established an azimuthal unconformity between near-latitudinal depressions and ridges that extend from MAR, on the one hand, and the WNW-trending transversal Cabo Verde Escarpment, on the other hand [3]. The seafloor in the studied test area is complicated by volcanic edifices and by the anomalously deep (>6000 m) Strakhov Basin trending in the NW direction discordantly relative to other structural units. The previously unknown Neva deepwater channel was also found (Fig. 3).

This paper has been prepared on the basis of the data collected during Cruise 16 of the R/V *Akademik Ioffe* in 2004. During this cruise, the sedimentary cover was studied with continuous seismic profiling (CSP). The structure of the upper part of the sedimentary cover and the bottom topography was investigated with a Parasound acoustic profilograph along a profile between $11.52^{\circ} \text{N} \times 22.67^{\circ} \text{W}$ and $10.13^{\circ} \text{N} \times 24.07^{\circ} \text{W}$ (Fig. 1). The structure of the upper part of the sedimentary cover in the Neva Channel and the Strakhov Basin was studied with the same method. The bedrock samples and cores of bottom sediments were recovered in the same place.

Structure of the sedimentary cover (based on CSP data). The CSP profile across the junction of continen-

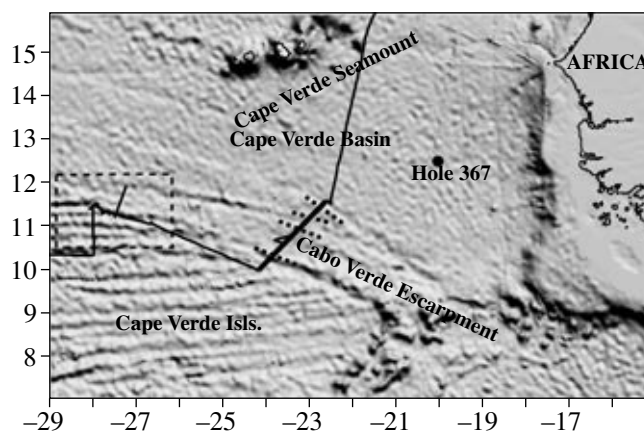


Fig. 1. Schematic map of works carried out at the junction of the southern end of the Cape Verde Seamount and the abyssal basin (based on the satellite altimetry data [9]). Solid lines show the survey routes during Cruise 16 of the R/V *Akademik Ioffe*; dashed lines, boundaries of test area of Cruise 22 of the R/V *Akademik Nikolai Strakhov*; heavy line, the location of seismic profile; dotted lines, axes of the ridges detected with the CSP; filled circle, DSDP Hole 367 (after [4]).

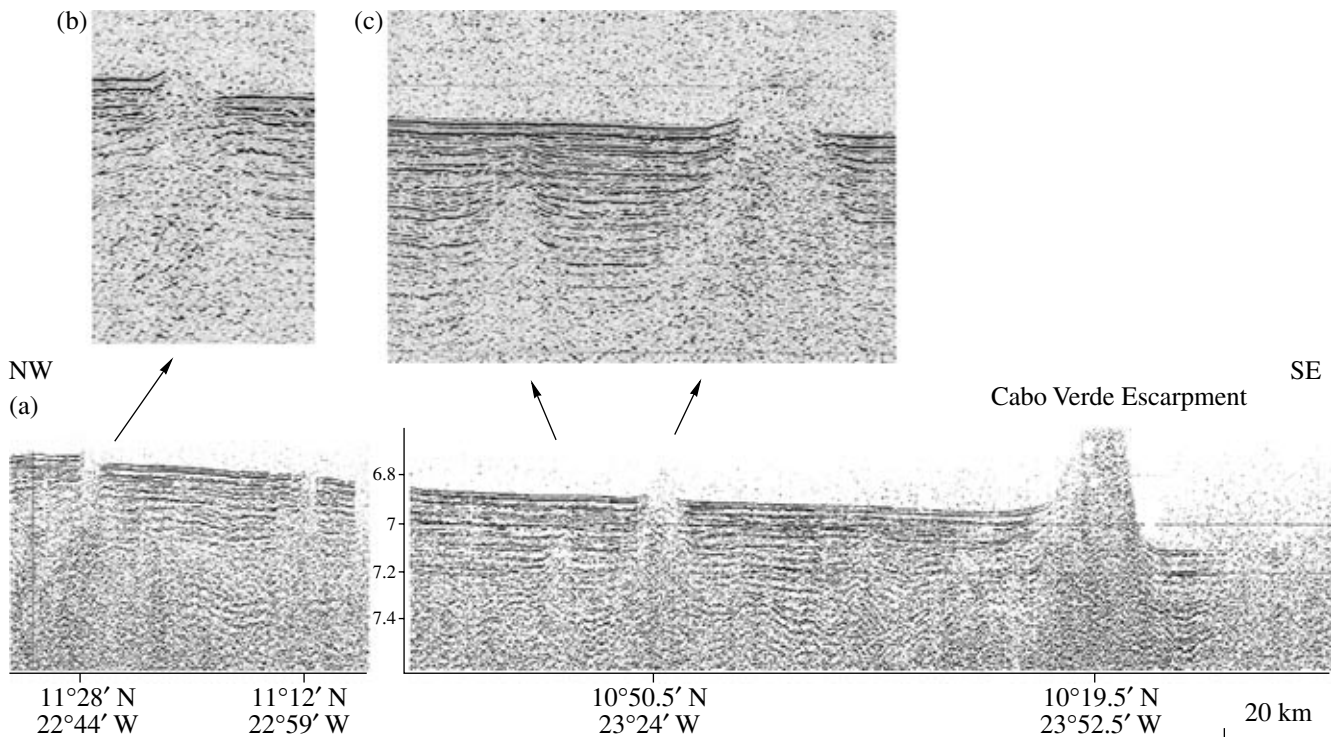


Fig. 2. Structure of sedimentary cover at the junction of the southern end of the Cape Verde Seamount and the abyssal basin along the seismic profile shown in Fig. 1. (a) Seismoacoustic time section obtained by the CSP team: V.G. Petrenko, O.A. Kuz'mina, and A.B. Khvoroshch, (Southern Division, Institute of Oceanology, Russian Academy of Sciences, Gelendzhik), V.N. Efimov (Geological Institute, Moscow), and S.A. Erofeev (Nizhni Novgorod Polytechnical University). Air guns of Pulse-6 type and one-channel streamer with working length of 25 m were used in the survey. The preliminary signal processing was performed by S.Yu. Sokolov (Geological Institute, Moscow) with a RadExPro v. 3.01 software package, DEKO GEOFIZIKA, Moscow State University. (b, c) Fragments of seismoacoustic records at rises and (c) buried inlier of seismoacoustic basement.

tal and oceanic structural units crossed the southern termination of the Cape Verde Seamount, the Cabo Verde Escarpment, and the adjacent structural features of the Cape Verde Basin. To the north of the Cabo Verde Escarpment, the seafloor is flat and slightly tilted to the southwest from a depth of 5040 to 5180 m near the Cabo Verde Escarpment. We can identify four bedded members in the time section (Fig. 2a), characterized by specific degree of stratification, amplitude of reflected signal, and so on (a detailed description will be presented in a special paper). Several inliers of acoustic basement are outlined. Some of them are buried beneath sediments, while other inliers tower above the seafloor as small seamounts 40–100 m high and 2–6 km wide at the floor (Figs. 2a, 2b, 2c). Some basement inliers have a block structure, whereas other inliers resemble truncated symmetric cones and probably represent paleovolcanoes. The Cabo Verde Escarpment (500 m high and ~20 km wide) has an asymmetric profile.

The maximum thickness of sedimentary rocks attains 1 km. All estimates of the sedimentary cover thickness were calculated from the assumption that the average seismic wave velocity in sedimentary sequences is 2 km/s.

Three upper members are similar in many parameters and generally characterized by a horizontal attitude of beds. Deformations of sediments are observed only near rises where the beds are either bent or deformed into small folds (Figs. 2b, 2c). One such rise separates the seafloor areas with different depths, suggesting normal or reverse faulting with an amplitude of about 30 m.

One of the larger folds, which envelop the buried basement inliers, is shown in the right part of Fig. 2c. The character of deformations of sediments above and near the inliers testifies to the vertical uplift of basement blocks.

The average thickness of the uppermost (first) member decreases southwestward from 100 to 50 m; the thickness of the second member, from 130 to 50 m. The average thickness of the third member is 90 m and as great as 230 m in depressions. Sediments of the fourth member fill depressions and make up synforms characterized by poor stratification. The internal boundaries are detected sporadically, indicating that the beds are deformed into gentle folds. The angular nonconformity is established between the fourth and the third members. The sedimentary units rest against the basement inliers.

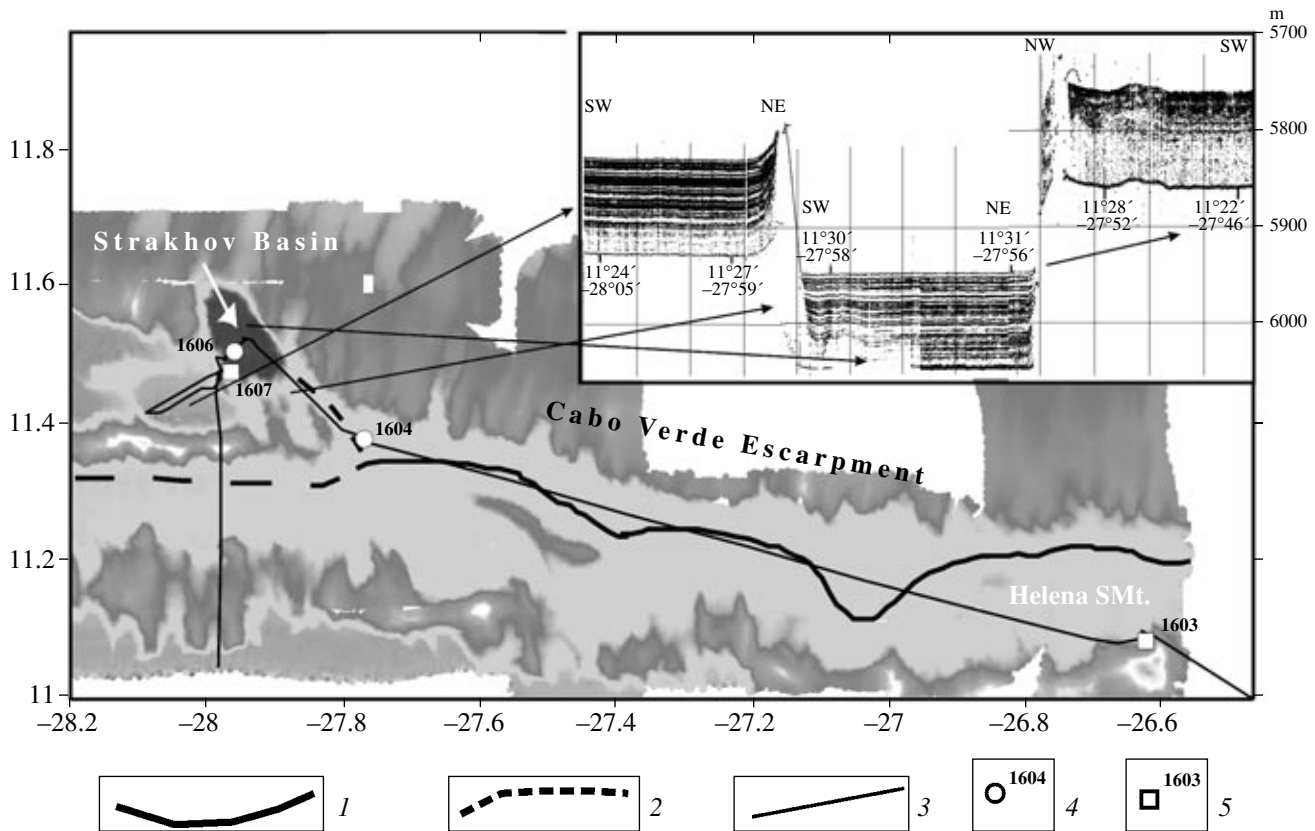


Fig. 3. Topography of the northern test area of Cruise 22 of the R/V *Akademik Nikolai Strakhov* (after [3]). (1) Neva Channel; (2) inferred extension of the channel; (3) traverses of the R/V *Akademik Ioffe*; (4) stations of bottom sediment sampling and their numbers; (5) stations of dredging and their numbers. The inset demonstrates the structure of the upper part of sedimentary cover in the Strakhov Basin and the adjacent areas (synthetic profile of a Parasound profilograph): a trough between the Strakhov Basin and the Neva Channel is shown on the right; the Strakhov Basin, in the center; and the depression located southwest of the Strakhov Basin, on the left.

The trough located south of the Cabo Verde Escarpment is a continuation of transform fracture zone. The trough floor lies approximately 130 m lower than the seafloor to the north of this escarpment. The thickness of the sedimentary cover in the trough (550–600 m) is markedly less than that of the sedimentary cover to the north of the Cabo Verde Escarpment. Four sedimentary members in the trough are distinguished by distinct stratification.

We correlated four units discernible in the seismo-acoustic time section with the sediments penetrated by the adjacent DSDP Hole 367 [4] (Fig. 1). The three upper members are correlated with the post-Early Miocene turbiditic marls, clays, and sands. The uppermost member is correlated with the Quaternary sediments. The total thickness of the sedimentary section is 320 m (~430 m in basins) and 290 m in the borehole. The oldest sedimentary rocks penetrated by DSDP Hole 367 overlie the basalts and are dated at the Early Jurassic. The Oligocene and lower Miocene beds have not been identified, probably, because a hiatus occurs in this stratigraphic interval. Hence, it may be supposed that the lowermost (fourth) member embraces the

Upper Jurassic–Eocene sedimentary rocks. However, we failed to subdivide this section into separate stratigraphic units.

Sedimentary cover in the Strakhov Basin and the Neva Channel. The deepwater Neva Channel, 10–15 km wide, is traced at the foot of the Cabo Verde Escarpment (Fig. 3). The depth of the entrenchment of the channel valley is 5–25 m, and local terraces are recorded on its slopes. The V-shaped channel profile in the east gives way to the U-shaped channel west of 27.5° W.

The Strakhov Basin is characterized by the flat floor and the thin-bedded cyclic sedimentary cover more than 100 m thick, distinguished by the maximum depth of acoustic signal penetration by Parasound (Fig. 3, inset). Cream-colored plastic clay with numerous clasts of Fe–Mn crusts was dredged from the slopes of the ridge that bounds the Strakhov Basin in the west (Station I1607, 11°28.50' N × 27°59.20' W, depth 5640–5470 m) (Fig. 3). The clay is a bedrock, because the wall of the Strakhov Basin is acoustically transparent on the Parasound echogram (Fig. 3, inset). The XRD results have shown that the clay consists largely of

palygorskite (d : 10.47, 6.39, 5.41, 4.48 Å), nontronite, and kaolinite.

Palygorskite was identified in samples taken during Cruise 1 of the R/V *Akademik Nikolai Strakhov* on the slopes of the Krylov Seamount, where this mineral metasomatically replaces hyaloclastite and alkali basalt. According to [5], this clearly indicates the hydrothermal origin of palygorskite.

The upper part of the sedimentary cover in the Strakhov Basin was sampled with a gravity corer (Station I1606, 11°30.15' N × 27°57.95' W, depth 5998 m) (Fig. 3). The sequence of greenish gray pelagic ooze, 350 cm in total thickness, is characterized by low carbonate content (0.41–13.81%) and a very fine grain size. The carbonate material consists of well-preserved nannoplankton, including *Pseudoemiliana lacunosa*, *Gephyrocapsa oceanica*, *Gephyrocapsa*, *Helicosphaera carteri*, and *Calcidiscus leptoporus*, which testify to the Pleistocene age of the sediments. Marcasite is abundant in the sediments.

The upper part of sedimentary section in the Neva Channel has been sampled at the site that adjoins the Strakhov Basin (Station I1604, 11°22.5' N × 27°46.3' W, depth 5770 m). The bedded unit of ooze and pelagic clay reaches 450 cm in thickness. The selected 35 beds differ in color, carbonate content, percentage of silt constituent and its composition, and in water content. The complex of nannoplankton similar with that at Station I1606 occurs at the base of the column.

The sediments formed in the slightly oxidized or reduced environments (Eh varies from +5 to +275 mV). The highest Eh values (>150 mV) are typical of the uppermost layer of oxidized sediments. The Eh values in sediments that fill the Strakhov Basin are somewhat lower than in sediments of the Neva Channel. This difference is also reflected in the composition of the gases dissolved in pore water. The gas was extracted from sediments using the standard technique and its composition was determined with a Crystal 2000m chromatograph. The concentration of nitrogen, the prevalent gas, reaches 98% in some samples. The methane concentration is within a range of 0.056–0.086% and increases with depth. However, at Station 1604, the CH₄ content is almost an order of magnitude lower than in the comparable units at Station 1606 in the Strakhov Basin.

Thus, the study of the upper sedimentary layer has shown a marked difference in sedimentation conditions and postsedimentary processes in the adjacent structural units. The uniform stagnant conditions of the closed deepwater Strakhov Basin resulted in the formation of homogeneous sequence of low-carbonate clay. In contrast, the multilayer sequence of clayey oozes with different carbonate contents was deposited in the Neva Channel in the running water environment as a result of active transport of sediments by bottom currents. The postsedimentary processes in the Strakhov Basin are more intense than in the Neva Channel, as evidenced by lower Eh values and elevated concentrations

of methane. This difference may be caused by different contents of organic matter buried in sediments and by multifold redeposition of sediments in the channel.

Composition of bedrocks. The bedrocks were dredged at Station I1603 (11°03.5' N × 26°37.1' W, depth 4800–4200 m) from the northern slope of the Helena Seamount, located on a near-latitudinal ridge in the test area (Fig. 3). The Fe–Mn crusts and nodules, gabbroic rocks, basalts, and sedimentary breccias have been dredged.

Basalts are aphyric and rarely plagiophyric. Both unaltered and strongly altered varieties are known. Plagioclase in the latter is replaced with saussurite, chlorite, and minerals of the epidote group. Clinopyroxene is almost completely replaced with actinolite and chlorite. The altered rocks are characterized by enrichment in water (1.4–6.9 wt %), K₂O, Rb, and U (as high as 1.5 wt %, 21.7, and 0.6 ppm, respectively). The loss of CaO reaches 4–8 wt %. The ferric component (6.3–6.5 wt % Fe₂O₃) in the altered rocks sharply prevails over the ferrous component (1.7–2.9 wt % FeO).

The basalts are similar to typical N-MORB [6] in composition, and characterized by low contents of TiO₂ (1.0–1.1 wt %), P₂O₅ (0.09–0.16 wt %), Y (18–28 ppm), Zr (53–56 ppm), Nb (1.6 ppm), Hf (1.4–1.5 ppm), Ta (0.1 ppm), and Th (0.09–0.10 ppm). However, an evolved sample demonstrates much higher contents of TiO₂ (1.8 wt %), P₂O₅ (0.19 wt %), Sr (160 ppm), Y (40 ppm), Zr (128 ppm), Nb (5.3 ppm), Hf (3.1 ppm), Ta (0.4 ppm), Th (0.3 ppm), and Ni (360 ppm). Basalts from Station I1603 are characterized by almost horizontal chondrite-normalized REE patterns (Fig. 4), typical of N-MORB.

The ratios of inert incompatible elements, such as Nb/Zr (0.03–0.04), Nb/Ta (13.4–14.7), and Ta/Th (1.1–1.3), in basalts are very low and indicate that the depleted asthenospheric mantle was their source [6].

The gabbroic rocks comprise olivine gabbro, gabbro, ore gabbro, and gabbroanorthosite composed of clinopyroxene, plagioclase, and olivine. The ore microgabbro consists of plagioclase, amphibole, and ilmenite as anhedral grains (up to 10%). All gabbroids are altered: olivine is replaced with serpentine; clinopyroxene is partly or completely replaced with amphibole; plagioclase is partly saussuritized and locally replaced with minerals of the epidote group occasionally associated with chlorite.

The ore gabbro is enriched in Ti and Fe and depleted in silica; elevated Na, K, and P contents are noteworthy. Gabbroanorthosite is characterized by extremely high alumina content and is markedly depleted in Fe and Mg. The chondrite-normalized REE curve of this rock is located much lower than that of basalt (Fig. 4). A positive Eu anomaly is typical, as takes place in rocks of the banded complex. The curve of one particular sample of ore gabbro corresponds to that of basalt. The ore microgabbro is distinguished by very high REE con-

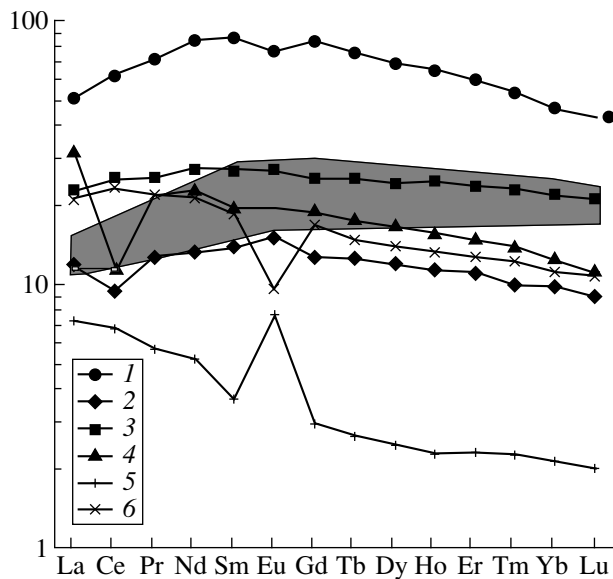


Fig. 4. Chondrite-normalized REE patterns of basalts and gabbroids. The field of N-MORB from the axial MAR zone between 10.6° N and 12° N [6] is shown by gray. (1, 6) Ore gabbro, (2, 3, 4) basalt, (5) gabbroanorthosite.

tents, and the respective curve is located much higher than the field of oceanic basalts, although the shape of the curve is similar to that of depleted tholeiites. The Eu minimum is distinctly expressed. Hence, the rock crystallized from a highly evolved melt, the initial composition of which was similar to N-MORB.

Plagioclase in gabbroic rocks mainly corresponds to An_{61-64} . Plagioclase is more calcic (An_{70-74}) in olivine gabbro and less calcic (An_{57}) in ore gabbro. Clinopyroxenes from all gabbroic varieties are similar to one another in the Fe ratio (FS_{44-45}) and in contents of TiO_2 (0.38–0.55 wt %), Al_2O_3 (3.12–3.91 wt %), Na_2O (0.35–0.63 wt %), and Cr_2O_3 (0.45–0.83 wt %). This composition is typical of clinopyroxene from oceanic gabbro.

The gabbroic rocks and basalts are comagmatic and characteristic of the oceanic lithosphere, especially of the igneous rocks that occur in the axial zone of MAR. They were formed under geodynamic conditions of spreading zones. Basalts are comparable with the rocks penetrated by DSDP Hole 367.

Fragments in the dredged breccia are composed largely of gabbroids that commonly underwent hydrothermal argillic alteration together with the cement.

CONCLUSIONS

As has been established, the Cabo Verde Escarpment divides the seafloor into areas with different types of topography and sedimentary cover. Judging from compositions of basalts and gabbroids, the seafloor to the southwest of the escarpment was formed in the

spreading setting. The total thickness of the three upper sedimentary members (post-Early Miocene–Quaternary sediments) increases in the northeastern direction away from the Cabo Verde Escarpment. This suggests that this escarpment was formed as a boundary of lithotectonic zones in the Oligocene–Early Miocene, when the Cape Verde Seamount was actively growing up [4].

In the process of the post-Early Miocene evolution, the tectonic movements at the southern end of the Cape Verde Seamount led to the uplift of inliers of acoustic basements and to the development of the Cabo Verde Escarpment with an amplitude reaching 200 m. These structural features spatially coincide with the WNW-trending ridges [9] that extend for many hundreds of kilometers. The Late Quaternary tectonic movements probably provided contrasting conditions of sedimentation in the study region. It may be suggested that in the Eocene, when volcanism was active [8], the hydrothermal processes resulted in the formation of palygorskite and argillic alteration of gabbroids.

ACKNOWLEDGMENTS

This work was fulfilled under the Program of Fundamental Research “Fundamental Problems of Oceanology: Geology, Physics, Biology and Ecology” supported by the Presidium of the Russian Academy of Sciences. The work was also supported by the Russian Foundation for Basic Research (project nos. 03-05-64159 and 05-05-65125) and the Federal Target Program “The World Ocean” (Subprogram “The Nature of the World Ocean”).

REFERENCES

1. A. O. Mazarovich, Dokl. Akad. Nauk **335**, 70 (1994).
2. Yu. M. Pushcharovsky, *Tectonics of the Atlantic with Elements of Nonlinear Geodynamics* (Nauka, Moscow, 1994) [in Russian].
3. A. O. Mazarovich, K. O. Dobrolyubova, V. N. Efimov, *et al.*, Dokl. Akad. Nauk **379**, 362 (2001) [Dokl. Earth Sci. **379A**, 615 (2001)].
4. Y. Lancelot, E. Seibold, P. Cepek, *et al.*, in *DSDP Initial Reports* (US Govt. Print. Office, Washington, DC, 1978), Vol. 41, pp. 21–326.
5. B. P. Zolotarev, V. A. Eroshechek-Shak, V. A. Gutsaki, and A. A. Richter, in *Volcanic Seamounts and Deepwater Sediments in the Eastern Central Atlantic* (Nauka, Moscow, 1989), pp. 95–111 [in Russian].
6. L. Dosso, H. Bougault, and J.-L. Joron, Earth Planet. Sci. Lett. **120**, 443 (1993).
7. J. Natland, in *DSDP Initial Reports* (US Govt. Print. Office, Washington, DC, 1978), Vol. 41, pp. 1107–1112.
8. A. O. Mazarovich, Geotektonika **32** (4), 53 (1998) [Geotectonics **32**, 296 (1998)].
9. D. T. Sandwell and W. H. F. Smith, J. Geophys. Res. **102** (B5), 10039 (1997).